Wetting and crystallization at grain boundaries: Origin of aluminum-induced crystallization of amorphous silicon

J. Y. Wang, D. He, Y. H. Zhao, et al.

🌐 **View Online**   ⬆ **Export Citation**

ARTICLES YOU MAY BE INTERESTED IN

Wetting and crystallization at grain boundaries: Origin of aluminum-induced crystallization of amorphous silicon

J. Y. Wang,[a] D. He,[b] Y. H. Zhao,[c] and E. J. Mittemeijer
Max Planck Institute for Metals Research, Heisenbergstrasse 3, D-70569 Stuttgart, Germany

It has been shown experimentally that the grain boundaries in aluminium in contact with amorphous silicon are the necessary agents for initiation of the crystallization of silicon upon annealing temperatures as low as 438 K. Thermodynamic analysis has shown (i) that Si can "wet" the Al grain boundaries due to the favorable Si/Al interface energy as compared to the Al grain-boundary energy and (ii) that Si at the Al grain boundaries can maintain its amorphous state up to a thickness of about 1.0 nm. Beyond that thickness crystalline Si develops at the Al grain boundaries. © *2006 American Institute of Physics*. [DOI: 10.1063/1.2172707]

Grain boundaries are known to effect solid-state diffusion and solid-state reactions. Usually, kinetic explanations for the phenomena observed are offered. In this work it is shown that such phenomena can have a thermodynamic, rather than kinetic origin. The paper demonstrates that "wetting" by and crystallization of silicon occurs at grain boundaries in a polycrystalline aluminium substrate and that both phenomena can be explained on a thermodynamic basis.

Bulk amorphous silicon crystallizes at a temperature of 960 K or higher.[1–3] This crystallization temperature can be significantly lower when the amorphous silicon phase is in intimate contact with metals with which they form eutectic phase diagrams, for example, Si/Au,[4] Si/Ag,[5] and Si/Al (Refs. 6 and 7) systems. No satisfactory, conclusive explanation for this phenomenon has been given until now; various, conflicting suggestions have been offered in the literature.[5–15] Here the thermodynamic reason for aluminium-induced crystallization of Si at grain boundaries within the Al phase will be given.

Sample A (and sample B) was prepared by sputter deposition of Al (50 nm) [and Al (150 nm)] and Si (150 nm) sublayer sequentially at room temperature in a high vacuum chamber in a single run onto a Si (510) substrate covered with an amorphous SiO_2 (50 nm) layer (as a diffusion barrier). Sample C was prepared as follows. The Al sublayer (50 nm) was first deposited onto a Al_2O_3 (0001) (sapphire) substrate at 573 K. Then the sample was annealed at 573 K for 2 h in order to reduce the Al grain-boundary density and to lower the total energy (e.g., strain energy) stored in the Al sublayer.[6] After slow cooling to room temperature and sputter cleaning of the surface of the annealed Al sublayer, the Si sublayer (150 nm) was deposited on top of the Al sublayer. The measured Al concentration-depth profiles at the Si/Al interface for the three as-deposited samples are identical (see below) and could be fitted by one single interface roughness parameter in the MRI model.[16] This result indicates that the annealing and sputter cleaning, performed for sample C after Al sublayer deposition, had no significant influence on the

surface morphology (interface roughness) and composition (interface contamination), as compared to samples A and B. For these three samples, the as-deposited Al and Si sublayers are polycrystalline and amorphous, respectively, as determined by x-ray diffraction (XRD) (see below). XRD and FIB (focused ion beam) measurements provided values of average grain size in the direction parallel to the surface equal to 50 nm, 230 nm, and 360 nm for samples A, B, and C, respectively. The annealing of the Al layer in sample C not only led to a much larger lateral grain size, but probably also led to more stable (e.g., low angle) grain boundaries.[17] Samples A, B, and C were finally annealed at 438 K for different times in an argon atmosphere in a Perkin-Elmer DSC-7 instrument. The concentration-depth profiles for the as-deposited and annealed samples were measured using a JEOL JAMP-7830F scanning Auger microscope. The XRD patterns were measured using a Philips MRD diffractometer and Cu $K\alpha$ radiation. Corresponding experimental details has been described elsewhere.[6,13]

The measured Al concentration-depth profiles for sample A (high grain-boundary density) as-deposited and annealed at 438 K for different times are shown in Fig. 1(a). A pronounced mass transfer across the original interface was observed after annealing for only 20 min and a new peak of Al concentration-depth profile appeared at the location of the original Si sublayer after annealing for 5 days. XRD measurements as shown in Fig. 1(b) indicate that upon continuous annealing of sample A the Si(111) diffraction peak of crystalline Si emerges at $2\theta=28.4°$ (Cu $K\alpha$ radiation); its integrated intensity increases with increasing annealing time. For sample B (lower grain-boundary density), a small amount of mass transfer was measured after annealing at 438 K for 30 min (see the inset in Fig. 2) and a small Si(111) diffraction peak of crystalline Si had emerged (see Fig. 2). For sample C (lowest grain-boundary density and low grain-boundary energy), even after annealing at 438 K for 5 days, no mass transfer and no diffraction peaks indicative of crystalline Si were measured at all as shown in Fig. 3. Evidently, as follows from both the Auger and XRD measurements, crystallization of amorphous silicon takes place only if apparent interdiffusion occurs and a gradual increase of Si crystallization kinetics becomes apparent as Al grain size is decreased.

---

[a] Author to whom correspondence should be addressed; electronic mail: j.y.wang@mf.mpg.de
[b] Current address: Department of Chemical Engineering and Applied Chemistry, University of Toronto, Toronto, Ontario M5S 3E5, Canada.
[c] Current address: Los Alamos National Laboratory, MS G755, MST-STC, Los Alamos, NM 87545.
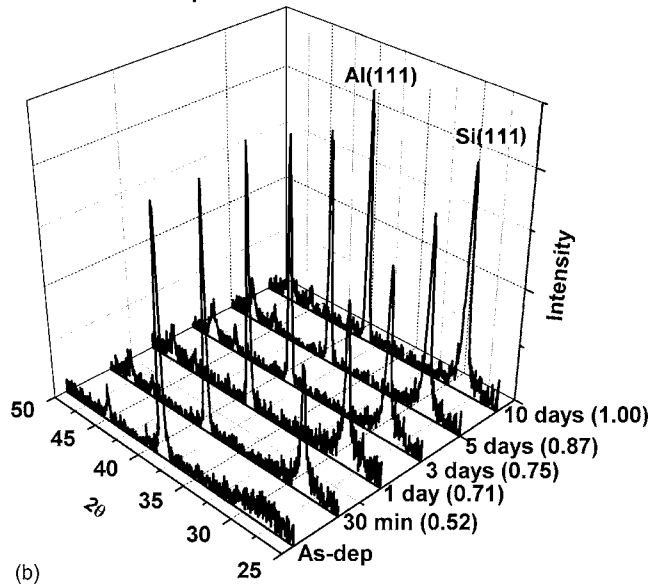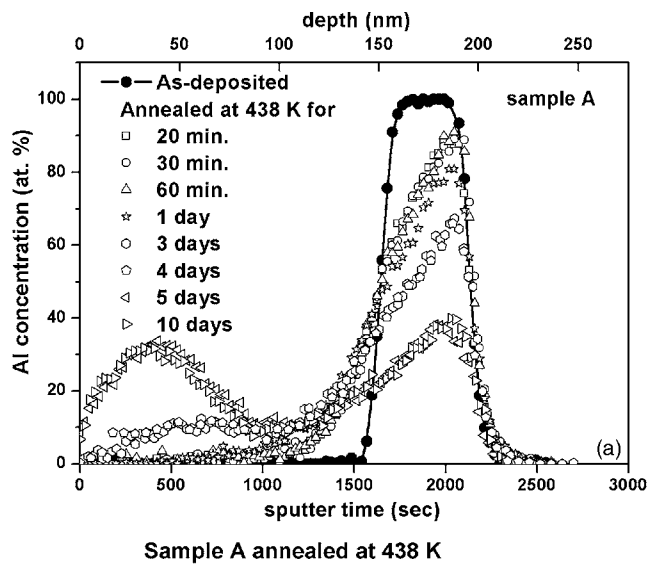
FIG. 1. (a) Al concentration-depth profiles and (b) XRD patterns (after subtraction of XRD background as recorded from the bare substrate) for as-deposited and annealed $Si(150 \, nm)/Al(50 \, nm)/SiO_2(50 \, nm)/Si(510)$ samples (A). The XRD measurements were performed under the same experimental conditions and using the same piece of sample A. The number within the brackets, after the time of annealing indication, represents a normalized value of the integrated intensity of the Si(111) peak.

There is no significant solid solubility of Al in Si and of Si in Al, and Si and Al do not form compounds.[18] Recent analysis of the apparent interdiffusion in Si/Al (multi)layer structures at temperatures down to 393 K has shown that the activation energy of this process is indicative of diffusion of Si along grain boundaries in Al.[13]

Hence, it is concluded: (i) interdiffusion in Si/Al is realized by diffusion of Si along grain boundaries in Al, and (ii) crystallization of Si is initiated at the grain boundaries in Al.

It has been suggested that a screening effect of the mobile electrons in Al on adjacent Si can occur, leading to a weakening of the covalent bonds of the adjacent Si.[19] These relatively weakly bonded Si atoms are called here "free Si" atoms, indicating that they may relatively easily migrate. Thus it is concluded that "free Si" atoms are induced at the interface of the Al and Si sublayers and may diffuse into Al along grain boundaries in Al. To understand why crystalliza-
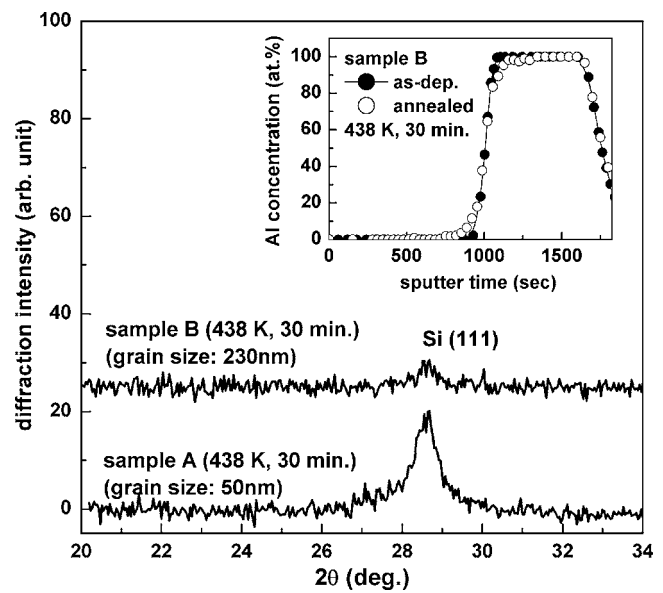

FIG. 2. XRD patterns (after subtraction of XRD background as recorded from the bare substrate) for $Si(150 \, nm)/Al(50 \, nm)/SiO_2(50 \, nm)/Si(510)$ sample (A) and $Si(150 \, nm)/Al(150 \, nm)/SiO_2(50 \, nm)/Si(510)$ sample (B) annealed at 438 K for 30 min. The inset shows the measured Al concentration-depth profiles for sample B as-deposited and annealed at 438 K for 30 min.

tion occurs at the grain boundaries in the Al sublayer, and not at the interface of the Al and Si sublayers, the following thermodynamic reasoning can be applied.

It had been shown for the first time in Refs. 20 and 21 that an amorphous layer can be thermodynamically stable if its thickness is below a critical value. Such stability is due to favourable interface energies for the amorphous layer as compared to those for the corresponding crystalline layer, which compensate the crystallization promoting difference in bulk energy of the amorphous and crystalline states of the layer. In the following calculation values for Al grain-boundary energy and interface energies are required for which no measured data exist. The Al grain-boundary energy and interface energies at 438 K have been calculated here
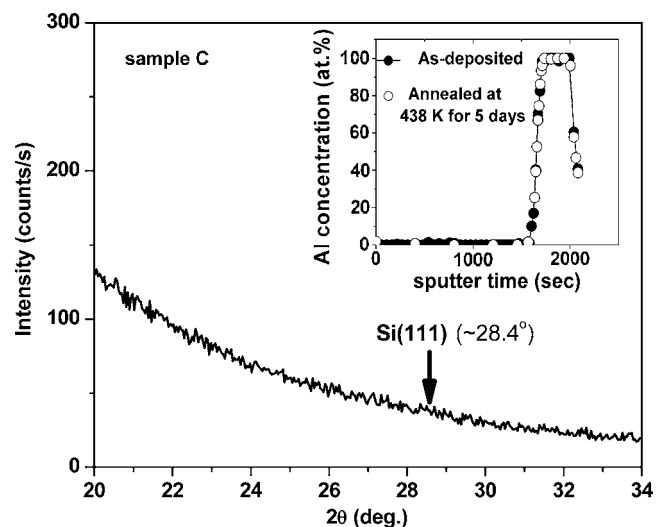

FIG. 3. XRD pattern [without subtraction of XRD background (!): cf. Fig. 2] for $Si(150 \, nm)/Al(50 \, nm)/Al_2O_3(0001)$ sample C as-deposited and annealed at 438 K for 5 days. The inset shows the measured Al concentration-depth profiles.

TABLE I. Calculated Si crystallization energy ($\Delta G_{\langle Si \rangle \text{-} \{Si\}}^{\text{crystallization}}$); Al grain-boundary energy ($\gamma_{\langle Al \rangle}^{\text{GB}}$); energies of the interfaces between crystalline Al and amorphous Si ($\gamma_{\langle Al \rangle / \{Si\}}^{\text{interface}}$), crystalline Al and crystalline Si ($\gamma_{\langle Al \rangle / \langle Si \rangle}^{\text{interface}}$) and crystalline Si and amorphous Si ($\gamma_{\langle Si \rangle / \{Si\}}^{\text{interface}}$) at 438 K.

$\Delta G_{\langle Si \rangle \text{-} \{Si\}}^{\text{Crystallization}}$ (J/m^3)	$\gamma_{\langle Al \rangle}^{\text{GB}}$ (J/m^2)	$\gamma_{\langle Al \rangle / \{Si\}}^{\text{interface}}$ (J/m^2)	$\gamma_{\langle Al \rangle / \langle Si \rangle}^{\text{interface}}$ (J/m^2)	$\gamma_{\langle Si \rangle / \{Si\}}^{\text{interface}}$ (J/m^2)
-8.3×10^8	0.344	0.036	0.454	0.095

along lines as explained detailedly in Refs. [6,20,21] The results have been listed in Table I.

Now consider the presence of an amorphous layer of ("free") Si (atoms) at a grain boundary in the Al layer. Firstly, the difference in interface (grain-boundary) energy, γ, upon inward diffusion of Si along an Al grain boundary (GB) is considered: $2 \times \gamma_{\langle Al \rangle / \{Si\}}^{\text{interface}} - \gamma_{\langle Al \rangle}^{\text{GB}}$, where $\langle \rangle$ and $\{ \}$ denote crystalline phase and amorphous phase, respectively. Using the data given in Table I, it is obtained $2 \times \gamma_{\langle Al \rangle / \{Si\}}^{\text{interface}} - \gamma_{\langle Al \rangle}^{\text{GB}} = -0.27$ J/m^2 (at 438 K). This result indicates that in any case a positive driving force occurs for "wetting" of the Al grain boundaries by Si and thus for the inward diffusion of Si along grain boundaries in Al.

Secondly, the maximal, critical thickness for an amorphous Si layer at a grain boundary in Al can be calculated, beyond which crystallization of this Si layer occurs. This critical layer thickness follows from

$$h_{\text{Al GB}}^{\text{critical}} = \frac{2 \times (\gamma_{\langle Al \rangle / \langle Si \rangle}^{\text{interface}} - \gamma_{\langle Al \rangle / \{Si\}}^{\text{interface}})}{-\Delta G_{\langle Si \rangle - \{Si\}}^{\text{crystallization}}},$$

where $\Delta G_{\langle Si \rangle - \{Si\}}^{\text{crystallization}}$ (J/m^3) is the crystallization energy of amorphous silicon at 438 K. Using the data given in Table I, it is obtained: $h_{\text{Al GB}}^{\text{critical}} = 1.0$ nm (at 438 K). This value equals about five monolayers of *a*-Si.

On a similar basis it may also be understood why crystallization does not occur at the Al/Si interface. The screening effect of the mobile electrons in Al on adjacent Si (see above) is of short-range nature and most likely restricted to 1–2 monolayers. The critical layer thickness for Si crystallization at the Al/Si interface follows from

$$h_{\langle Al \rangle / \{Si\}}^{\text{critical}} = \frac{\gamma_{\langle Al \rangle / \langle Si \rangle}^{\text{interface}} + \gamma_{\langle Si \rangle / \{Si\}}^{\text{interface}} - \gamma_{\langle Al \rangle / \{Si\}}^{\text{interface}}}{-\Delta G_{\langle Si \rangle - \{Si\}}^{\text{crystallization}}}.$$

Using the data given in Table I, it is obtained: $h_{\langle Al \rangle / \{Si\}}^{\text{critical}} = 6.0$ nm (at 438 K). This value equals about three monolayers of *a*-Si. Hence, the layer of 1–2 monolayers of "free" Si at the Al/Si interface is too thin to crystallize.

It is remarked that the reason of absence of any crystallization of silicon in sample C, after 5 days at 438 K, may not only be the relatively low Al grain-boundary density of sample C, but also the relatively low energy of the Al grain boundaries remaining after the initial anneal of the as-deposited Al sublayer: a low value of Al grain-boundary energy obviously decreases the driving force for "wetting" of the Al grain boundaries by Si [the estimate made three paragraphs above pertains to a high angle grain boundary in Al (Ref. 20)].

In summary, aluminium-induced crystallization of silicon starts with inward diffusion of Si along grain boundaries in aluminium, because a positive driving force for "wetting" the Al grain boundaries exists. Subsequent crystallization of the Si can occur if the Si layer at the Al grain boundaries exceeds a critical thickness, which is of the order of five atomic layers.

[1] E. P. Donovan, F. Spaepen, D. Turnbull, J. M. Poate, and D. C. Jacobson, J. Appl. Phys. **57**, 1795 (1985).
[2] J. C. C. Fan and C. H. Andeson, Jr., J. Appl. Phys. **52**, 4003 (1981).
[3] Y. Tatsumi, M. Hirata, and K. Yamada, J. Phys. Soc. Jpn. **50**, 2288 (1981).
[4] J. R. Bosnell and U. C. Voisey, Thin Solid Films **6**, 161 (1970).
[5] T. J. Konno and R. Sinclair, Mater. Sci. Eng., A **179/180**, 426 (1994).
[6] Y. H. Zhao, J. Y. Wang, and E. J. Mittemeijer, Appl. Phys. A **A79**, 681 (2004).
[7] E. Pihan, A. Slaoui, P. Roca, i. Cabarrocas, and A. Focsa, Thin Solid Films **451–452**, 328 (2004).
[8] J. Klein, J. Schneider, M. Muske, S. Gall, and W. Fuhs, Thin Solid Films **451–452**, 481 (2004).
[9] O. Nast and S. R. Wenham, J. Appl. Phys. **88**, 124 (2000).
[10] Y. Masaki, T. Ogata, H. Ogawa, and D. I. Jones, J. Appl. Phys. **76**, 5225 (1994).
[11] M. S. Ashtikar and G. L. Sharma, J. Appl. Phys. **78**, 913 (1995).
[12] T. J. Konno and R. Sinclair, Philos. Mag. B **66**, 749 (1992).
[13] J. Y. Wang, A. Zalar, and E. J. Mittemeijer, Appl. Surf. Sci. **222**, 171 (2004).
[14] M. S. Haque, H. A. Naseem, and W. D. Brown, J. Appl. Phys. **75**, 3928 (2000).
[15] P. I. Widenborg and A. G. Aberle, J. Cryst. Growth **242**, 270 (2002).
[16] J. Y. Wang and E. J. Mittemeijer, J. Mater. Res. **19**, 681 (2004).
[17] M. J. Rost, D. A. Quist, and J. W. M. Frenken, Phys. Rev. Lett. **91**, 026101 (2003).
[18] J. L. Murray and A. J. McAlister, Bull. Alloy Phase Diagrams **5**, 74 (1984).
[19] A. Hiraki, Surf. Sci. Rep. **3**, 357 (1984).
[20] R. Benedictus, A. Böttger, and E. J. Mittemeijer, Phys. Rev. B **54**, 9109 (1996).
[21] L. P. H. Jeurgens, W. G. Sloof, F. D. Tichelaar, and E. J. Mittemeijer, Phys. Rev. B **62**, 4707 (2000).